DENTAL MATERIALS 35 (2019) 98–104

Available online at www.sciencedirect.com

ScienceDirect

journal homepage: www.intl.elsevierhealth.com/journals/dema

Strength-limiting damage in lithium silicate glass-ceramics associated with CAD–CAM

Dan L. Romanyk[a,1], *Ysidora Torrealba Martinez*[a,1], *Sydney Veldhuis*[a], *Nyssa Rae*[a], *Yilan Guo*[a], *Slobodan Sirovica*[a], *Garry J.P. Fleming*[b], *Owen Addison*[a,*]

[a] *University of Alberta, School of Dentistry, Edmonton, AB, Canada*
[b] *Materials Science Unit, Dublin Dental University Hospital, Lincoln Place, Dublin 2, Ireland*

ARTICLE INFO

Article history:
Received 29 August 2018
Received in revised form
15 October 2018
Accepted 1 November 2018

Keywords:
CAD–CAM
Strength
Lithium silicate ceramic
Fracture
Machining

ABSTRACT

Objective. The fabrication of all-ceramic restorations using Computer Aided Design and Computer Aided Manufacturing (CAD–CAM) most commonly involves subtractive machining which results in strength-limiting, surface and sub-surface damage in the resultant prosthesis. The objective was to explore how clinically relevant machining-process variables, and material variables, affect damage accumulation in lithium silicate glass-ceramics.

Methods. Three commercial lithium silicate glass-ceramics (IPS e.max® CAD, Celtra® Duo and Vita Suprinity®) were selected. For each material, two groups of disk-shaped specimens were fabricated (n = 15), using a CAD–CAM process, creating surfaces equivalent to those generated for a dental restoration, or alternatively, using a highly controlled laboratory process generating disk-shaped test specimens with a consistent polished surface. Bi-axial flexure strength (BFS) was determined in a ball-on-ring configuration and fractographic analyses performed. For each material BFS was correlated with machining sequence and with surface roughness.

Results. BFS was significantly influenced by material substrate ($p < 0.01$) and by fabrication route ($p < 0.01$). A significant factorial interaction ($p < 0.01$) identified that the magnitude of changes in BFS when comparing the two specimen fabrication routes, was dependent on substrate type. The polished control specimens exhibited a significantly increased BFS when compared with the CAD–CAM counterparts for all materials. IPS e.max® CAD and Celtra® Duo showed a 44 and 46% reduction in mean BFS for the CAD–CAM specimens when compared with the polished counterparts, respectively. In contrast, Vita Suprinity® showed the least disparity in mean BFS (21%) but the greatest variance in BFS data.

Significance. All CAD–CAM specimens showed evidence of machining introduced damage in the form of median and radial cracks at sites either coincident with, or peripheral to the failure origin. Subtractive machining introduced significant strength limiting damage that is not eliminated by heat treatments applied for either microstructure development (IPS e.max® CAD and Vita Suprinity®) or annealing/crack blunting (Celtra® Duo).

* *Corresponding author at*: University of Alberta, School of Dentistry, Edmonton Clinic Health Academy, Edmonton, AB, T6G 1C9, Canada.
E-mail address: oaddison@ualberta.ca (O. Addison).
[1] Co first authors.

https://doi.org/10.1016/j.dental.2018.11.004
0109-5641/

1. Introduction

The fabrication of all-ceramic dental restorations using Computer Aided Design and Computer Aided Manufacturing (CAD–CAM) most commonly involves subtractive machining [1]. Ceramic blocks of a uniform composition and microstructure [2] are shaped to a planned geometry using a multipoint contact grinding process [3]. Almost universally in dentistry, rotating burs with embedded diamond particles are used as the abrasive machining tool [1]. When contact is made between the hard irregular diamond particles and the ceramic surface, localized stress concentration occurs resulting in micro-fracture and material loss [3–5]. In polycrystalline materials, micro-cracks extend along grain boundaries dislodging small volumes of material [6,7]. In poly-phase materials such as dental glass-ceramics, the crack propagation associated with material removal is less predictable and is microstructure dependent [7,8]. For relatively low toughness glass-ceramics such as leucite-reinforced glass (fracture toughness of between 1–1.5 MPa.$m^{1/2}$ [9]), cracks can extend through both amorphous and crystalline phases [8]. In contrast, for lithium silicate glass-ceramics (fracture toughness >2.0 MPa $m^{1/2}$ [9]), crack propagation occurs almost exclusively within the glass matrix [8]. Although these micro-fracture events are a pre-requisite for the shaping of the prosthesis, the contact between the machining tool and the ceramic surface also results in damage which limits the strength of the machined object [3,7,10–12].

The type of damage generated in ceramic materials as a result of grinding and polishing is well understood. Contact between the abrasive and the ceramic introduces both strength limiting cracks and plastic contact damage resulting in residual stresses localized within a region near the machined surface [3,5,7,11]. Material strength is subsequently determined by the severity of the strength-degrading cracks and their interaction with the residual stress field [3]. Fractographic analyses identified two principal crack populations associated with the abrasive machining of ceramic materials [3,11–14]. Median cracks are formed parallel to the direction of motion of the abrasive contact and extend into the ceramic bulk (Fig. 1). Median cracks are not isolated, but rather can be considered as a series of adjoining, or coalescing, semi-elliptical defects extending from beneath the plastically deformed zone [3]. In contrast, lateral cracks are formed normal to the grinding direction and are typically less severe than the median cracks with a reduced influence on strength [5] (Fig. 1).

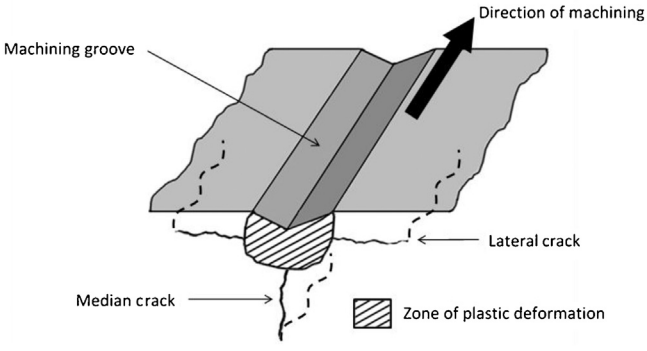

Fig. 1 – Schematic representation of damage accumulation on a ceramic surface associated with abrasive grinding.

Both crack populations are influenced by a residual stress field which manifests as a crack wedging force beneath the machining groove and a compressive crack stabilizing force adjacent to the groove [3]. Material strength is subsequently determined by the severity of the strength-degrading cracks and a variable interaction with residual stress fields [3,5]. Therefore, significant deviations arise when comparing fracture strength data with failure stresses predicted when cracks are modeled as a 'Griffith' flaw [3]. The introduction of residual stresses which can act to either stabilize or extend cracks, is dependent on both material and machining parameters, but there is evidence to suggest that crack stabilizing compressive stresses remain confined to a relatively shallow surface layer less than the median crack length [3].

The use of CAD–CAM to fabricate all-ceramic dental restorations is increasing; however, technology evaluations have mainly focused on outcome measures such as machining accuracy [15] as opposed to the manufacturing-process dependent variables that influence the fracture resistance of the all-ceramic restoration. It is acknowledged that both surface and subsurface damage introduced during machining results in a significant disparity between the measured strength of the machined ceramic object and the strength of the material in its un-machined state [12,16,17]. The impact that substrate (ceramic microstructure) and process (machining tool degradation or post-machining thermal treatment) specific variables have on the extent of strength limiting damage left by abrasive machining is poorly understood. Previously it was shown that CAD–CAM of a feldspathic dental ceramic introduces considerable variability in the surface roughness and the nature of the strength limiting defects, with strength-limiting flaw generation being independent of the machining sequence and tool degradation [12]. For a relatively low toughness glass-ceramic (leucite reinforced), it has been shown that alteration of the machined surface by polishing results in a substantial strength increase [18]. The strength modification can be attributed to the removal or reduction in length of the critical surface defects and changes to the surface residual stress state by polishing [19,20].

Currently, the most common substrates used for 'chairside' CAD–CAM fabrication of all-ceramic restorations are lithium silicate glass-ceramics. Several lithium silicate materials are available commercially, differing both in their microstructure and processing route, either being machined in a partially crystallized state or in a relatively harder fully crystallized state. The aim of this study was to explore how clinically relevant machining-process and material variables influence damage accumulation and strength degradation in lithium silicate-based glass-ceramics. The hypothesis tested was that the biaxial flexure strength (BFS) of lithium silicate glass-ceramics fabricated by a clinically relevant CAD–CAM process would be significantly lower than that of equivalent test objects manufactured using routine laboratory testing methods.

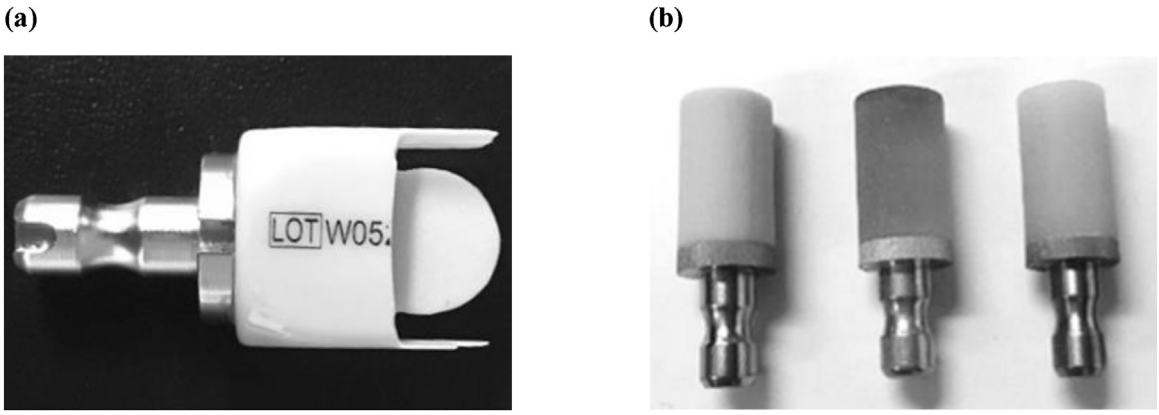

Fig. 2 – Image of (a) CAD–CAM block partially machined to produce a disk-shaped specimen for BFS testing and (b) water-jet machined ceramic blocks shaped into cylinders for the fabrication of control specimens.

2. Materials and methods

2.1. *Lithium silicate substrates*

Three commercially available lithium silicate glass-ceramics were selected. IPS e.max® CAD (Lot# W05269, Ivoclar Vivadent Inc., Schaan, Litchenstein); Vita Suprinity® (Lot# 43904, Vita Zahnfabrik, DE); and Celtra® Duo (Lot# 18028463, Dentsply Sirona, USA) were sourced in the form of 12 × 14 × 18 mm (width × thickness × length) pre-fabricated blocks for use in 'chair-side' dental CAD–CAM unit (Sirona CEREC MC X, Dentsply Sirona, USA). IPS e.max® CAD, a lithium di-silicate glass-ceramic, is presented in a partially crystallized state and receives a thermal treatment after machining to complete crystallization. Vita Suprinity® is described as a zirconia reinforced lithium silicate glass-ceramic, where the zirconia reinforces the glass matrix [21]. In common with IPS e.max® CAD, Vita Suprinity® is machined in a partially crystallized state and is subsequently heat treated to achieve full crystallization. Celtra® Duo is also a zirconia reinforced lithium silicate glass-ceramic, but, in contrast to IPS e.max® CAD and Vita Suprinity®, is machined in a harder fully crystallized form. A heat treatment is recommended following machining; however, heating does not result in changes to the crystalline phase of the microstructure [22].

2.2. *Specimen manufacture*

For each material, two groups of disk-shaped specimens were fabricated (n = 15 per group). One group utilized a CAD–CAM process creating surfaces equivalent to those generated for a dental restoration. Alternatively, a highly controlled laboratory process aimed at generating disk-shaped test specimens with a consistent polished surface finish was used for the second group. Nominally identical CAD–CAM fabricated disks (10 mm diameter and 1 mm thickness) were fabricated according to a previously reported method [12]. Briefly, a disk-shaped mold of equivalent dimensions was scanned with a CEREC Omnicam (Dentsply Sirona, USA). A single flat disk-shape geometry was designed in the CEREC v4.5 software. Disks were machined from pre-fabricated blocks in a two-axis 'chair-side' dental CAD–CAM unit (Sirona CEREC MC X) for each of the three substrate materials (Fig. 2a). New diamond particle burs, one stepped and one cylindrical, were installed on the milling machine before machining of a new substrate type commenced. Each CAD–CAM disk-shaped specimen was labeled to allow the machining sequence to be recorded. In the event a bur failed before an individual group size of n = 15 was completed, a new bur was introduced. Machining left a small residual 'tab' at the disk edge continuous with the upper surface. The upper surface was marked, to allow consistent orientation during mechanical testing, and the 'tab' manually removed using abrasive paper prior to testing.

For each material, a control group (n = 15) was generated by firstly reducing the pre-fabricated ceramic blocks to 10 mm diameter cylinders, using a water-jet machining process (Fig. 2b). Cylinders were then sectioned transversely using an IsoMet 5000 precision saw with a diamond particle cutting blade (Buehler, USA) with an average feed rate of 4.0 mm/min and a blade speed of 300 rpm, with water lubrication, to generate disk samples of 1.00 ± 0.10 mm thickness.

Following machining, both CAD–CAM and control disk-shaped specimens were subjected to a thermal treatment according to individual substrate manufacturer's recommendations. Crystallization of the IPS e.max® CAD specimens was completed in an Ivoclar Vivadent Programat EP 5000 furnace. Specimens were pre-heated at 403 °C for 6 min; the temperature was increased at 90 °C/min to 820 °C (under vacuum from 550–820 °C), held for 0.1 min and then increased under vacuum at 30 °C/min to 840 °C and held for 7 min, prior to long term cooling from 700 °C. Crystallization of Vita Suprinity® was completed in a VITA Vacumat 6000 MP furnace. Specimens were pre-heated at 400 °C for 4 min; the temperature was increased at 55 °C/min to 840 °C under vacuum, held for 8 mins, prior to long term cooling from 680 °C. Celtra® Duo which is fully sintered was heat treated in an Ivoclar Vivadent Programat EP 5000 furnace. Specimens were pre-heated at 500 °C for 2 min; the temperature was increased at 60 °C/min to 820 °C, held for 1 min, prior to long term cooling from 750 °C. Following thermal treatments, one surface of each of the control specimens (the uppermost in the furnace) was manually polished sequentially with SiC abrasive papers, using sequen-

tially P800, P1000, P1500 and P2000 grits, for 90 s per grade, with water lubrication to create a consistent surface finish.

2.3. Biaxial flexure strength (BFS) determination

The BFS of each disk-shaped specimen was determined in a ball-on-ring configuration using an ElectroPuls E3000 (Instron, USA) universal testing apparatus. Disk-shaped specimens were supported on an 8.3 mm diameter knife-edge ring support and loaded centrally with a 7.9 mm diameter stainless steel indenter at a cross-head speed of 1 mm/min. CAD–CAM specimens were oriented with the marked 'upper' surface in contact with the indenter. The control specimens were oriented so that the polished surface was in tension. BFS (MPa) was calculated using a Timoshenko and Woinowsky Krieger formula [20] (Eq. (1)):

$$BFS = \frac{P}{h^2} \cdot \left[(1+\upsilon) \cdot \left[0.485 \cdot \ln\left(\frac{a}{h}\right) + 0.52\right] + 0.48\right] \quad (1)$$

where, P was the force at fracture (N), ν was the Poisson's ratio for the material, a was the radius of the knife-edge support (mm), and h was the sample thickness (mm). Sample thickness was calculated as the mean of the measured dimensions at the fracture faces of all fracture fragments generated during testing (measured using a screw-gauge micrometer with precision of 10 μm). The values for Poisson's ratio were individually assigned as $\nu = 0.215$ for IPS e.max® CAD, $\nu = 0.208$ for Vita Suprinity®, and $\nu = 0.222$ for Celtra® Duo [23].

2.4. Surface metrology

To discriminate differences in the surface roughness generated between specimen groups, an optical profilometer (Nexview 5000, Zygo, USA) was used to calculate a mean Ra-value from a 2D measurement area randomly chosen close to the center of each disk-shaped specimen. A 10× Mirau objective lens was used with a magnification of 2.0×, providing a resolution of 0.1 nm in the z-axis. Mean Ra-value was determined from a rectangular measurement area of 0.36 × 0.27 (x vs y) mm.

2.5. Scanning electron microscopy (SEM) and failure analysis

Fracture fragments generated from BFS testing were selected corresponding to low and mid strength failures from each specimen group. Fracture fragments were sputtered with a 7 nm Au/Pd coating and fracture surfaces imaged in a Hitachi S-4800 SEM (Hitachi High-Technologies, Japan) at 200× magnification with an operating voltage of 5 kV. Resultant images were qualitatively analysed to identify fracture origins and evidence of fabrication associated surface damage.

2.6. Statistical analysis

A two-way ANOVA was used to determine differences in BFS between groups ($\alpha = 0.05$) where the factors were substrate material (at three levels) and fabrication route (at two levels). Post-hoc Tukey tests ($\alpha = 0.05$) were used to determine differences between BFS of the different substrate materials. An equivalent statistical approach was used to determine differences in surface roughness (Ra-value).

Table 1 – Mean BFS and surface roughness (mean Ra-value) with associated standard deviations. Common superscripts denote no significant difference between groups at $\alpha = 0.05$.

Material	Control		CAD–CAM	
	BFS (MPa)	Ra (nm)	BFS (MPa)	Ra (nm)
IPS e.max® CAD	643 ± 86^{a}	$59 \pm 25^{\#}$	362 ± 24^{c}	$4141 \pm 887^{*}$
Vita Suprinity®	405 ± 121^{b}	$46 \pm 21^{\#}$	$321 \pm 65^{b,c}$	$3191 \pm 866^{*}$
Celtra® Duo	409 ± 81^{b}	$62 \pm 22^{\#}$	220 ± 16^{d}	$4566 \pm 642^{*}$

Different superscript letters (a–d)indicate statistical differences in BFS ($p < 0.05$) & Different symbols (*,#) indicate statistical differences in Ra-value ($p < 0.05$)

3. Results

A two-way ANOVA demonstrated that BFS was significantly influenced by material substrate ($p < 0.01$) and by machining route ($p < 0.01$). A significant factorial interaction ($p < 0.01$) identified that the magnitude of changes in BFS when comparing the two specimen fabrication routes, was dependent on substrate type. Mean BFS and associated standard deviations are summarized in Table 1. Post-hoc Tukey tests demonstrated that IPS e.max® CAD exhibited a significantly higher mean BFS than both Vita Suprinity® ($p = 0.04$) and Celtra® Duo ($p < 0.01$). The polished control specimens were significantly stronger when compared with their CAD–CAM counterparts for all materials. Vita Suprinity® showed the least disparity in mean strength (21%) when comparing specimens with a highly polished surface with the clinically relevant CAD–CAM generated surface. IPS e.max® CAD and Celtra® Duo showed a 44 and 46% reduction in BFS for the machined specimens, respectively. No significant differences in the surface roughness (mean Ra-value) were observed between the three materials for an equivalent fabrication route ($p < 0.01$) (Table 1). For the CAD–CAM fabricated specimens, there was no clear relationship between the machining sequence and BFS for all substrates studied (Fig. 3).

The polished control test specimens exhibited greater variance about the mean BFS value when compared with the CAD–CAM fabricated specimens and is seen as greater spread of the BFS data in Fig. 4. Both IPS e.max® CAD and Celtra® Duo groups fabricated by CAD–CAM exhibited low relative standard deviations (RSD) of 6.6 and 7.3%, respectively. In contrast, CAD–CAM Vita Suprinity® exhibited a higher RSD of 20%.

Representative SEM images of the fractures surfaces of CAD–CAM fabricated specimens are shown in Fig. 5a–c with the fracture origins marked. All examined specimens showed evidence of machining introduced damage in the form of median and radial cracks at sites either coincident with or peripheral to the failure origin. In general, surface damage for IPS e.max® CAD was confined to a depth <50 μm (Fig. 5a). For low strength Vita Suprinity® CAD–CAM specimens (Fig. 5b), evidence of lateral cracking was seen at a depth of 40–80 μm from the machined surface. For Celtra® Duo CAD–CAM speci-

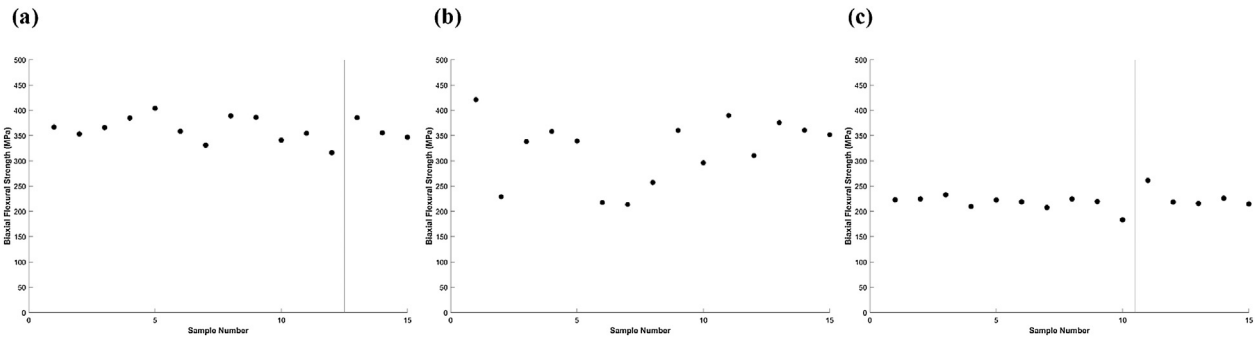

Fig. 3 – Association between milling sequence (sample number) and BFS for CAD–CAM fabricated (a) IPS e.max® CAD, (b) Vita Suprinity® and (c) Celtra® Duo sample groups. A vertical line represents a change in bur following machining tool breakage during milling. A new bur set was installed at the onset of milling each sample group.

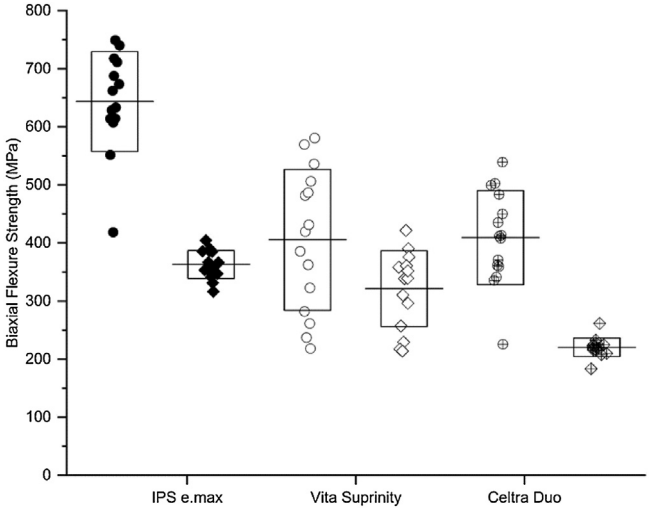

Fig. 4 – Box plots showing the mean BFS (MPa) and one standard deviation, overlaid on all data for groups of IPS e.max® CAD, Vita Suprinity® and Celtra® Duo samples manufactured either by CAD–CAM (diamonds ♦) or using a controlled process to introduce a highly polished surface finish (circles ●).

mens (Fig. 5c), median and radial cracks were observed up to depths exceeding 100 μm from the surface.

4. Discussion

For each lithium silicate glass-ceramic studied, the BFS of the CAD–CAM specimens was significantly lower than that of the substrate-matched control (Fig. 4). The control specimens exhibited a highly polished surface (~70-fold decrease in mean Ra-value compared with the CAD–CAM samples) which is typical of the surface finish introduced onto dental ceramic test objects for many in-vitro studies [23–25]. By using polishing to restrict the size of surface defects, investigators risk reporting exaggerated and clinically irrelevant material strengths. Surface defect integral relevance can be ensured by matching clinical restoration fabrication processes when making mechanical test specimens. For CAD–CAM ceramics, many investigators have reported load-to-failure data of test objects in an equivalent geometry to a dental restoration — employing the so called 'crunch-the-crown' approach [26,27]. Although the surface condition is equivalent to that of the clinical prosthesis, the test itself is limited as failure stresses cannot be calculated, clinically encountered fracture patterns are not observed, and unrealistic forces are required to initiate fracture [27]. In this study, these shortfalls were overcome by testing planar specimens which had been fabricated by CAD–CAM, thereby allowing calculation of failure stresses

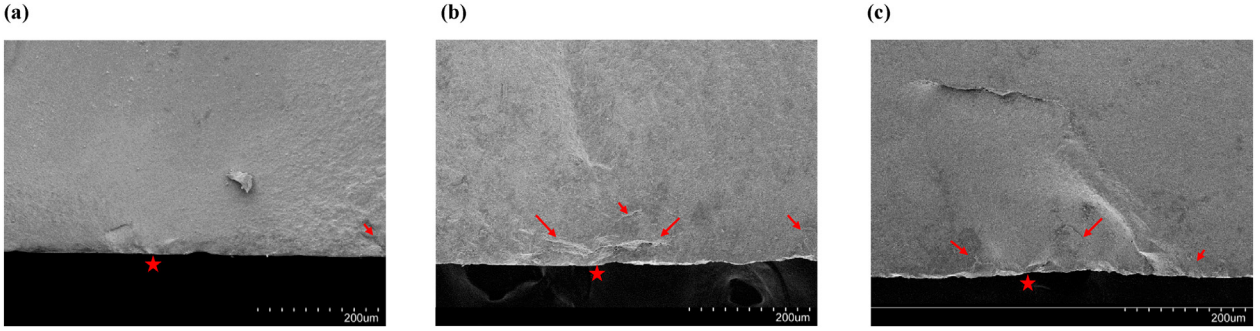

Fig. 5 – Scanning electron micrographs showing representative fracture surfaces derived from BFS testing of (a) IPS e.max® CAD, (b) Vita Suprinity® and (c) Celtra® Duo, manufactured using CAD–CAM. Fracture origins are indicated (⋆) and machining associated damage in the form of radial and sub-surface median cracks identified (→).

from objects possessing equivalent surface and sub-surface damage to the actual restoration. Fractographic analyses, confirmed that the types of defects observed on the fracture surface of the CAD–CAM test specimens (median and lateral cracks associated with plastic deformation) were entirely consistent with the expected pattern of damage accumulation associated with abrasive grinding of ceramic materials [3].

Whilst all three lithium silicate materials exhibited a reduced BFS when fabricated by a CAD–CAM process when compared with the polished controls, the pattern of the strength decrease differed. For IPS e.max® CAD and Celtra® Duo, the low variance in the fracture strength data suggests a relatively consistent strength limiting surface defect integral exists following crystallization or heat treatment, respectively. When considering material selection, this is important as the low variance in system strength should allow predictable usage when taken into context with the mean strength. In contrast, Vita Suprinity® exhibited a much higher variance in BFS, for both CAD–CAM and control fabricated test specimens implying greater variability in the size and distribution of strength limiting defects. In common with a previous study [12], no correlation between test specimen machining sequence, analogous to increasing machining tool usage, was observed for any of the three substrates employed. Machining tool deterioration, including plucking of abrasive particles, has been shown previously and is likely to impact on machining efficiency [12,28]. However, in this study no direct control over machining parameters such as feed-rate or cutting force was possible and therefore the influence of these factors, considered in combination with tool deterioration, could not be systematically explored.

The BFS of the CAD–CAM specimens is dependent on both the initial damage introduced by machining and the post-machining heat treatments which were used to develop the microstructure and/or modify pre-existing surface defects by annealing or crack blunting [12,29]. It has previously been shown that microstructural characteristics have a dominant influence on a ceramic materials' response to machining and to the associated degradation in strength [7]. In this study, Celtra® Duo was machined in a fully crystallized state whereas IPS e.max® CAD and Vita Suprinity® were machined in a pre-crystallized more glassy state. For the two conditions, differences will exist in both the cutting forces required to dislodge material and in the dominant mechanism of material removal, with both factors understood to impact on strength [7]. In general, increasing grain size favors grain dislodgment or cleavage of coalesced grains removing material by chip formation rather than plastic flow [5,7] and requires reduced cutting forces. For an equivalent material reducing the cutting forces will lessen the impact on strength degradation [5]. However, material removal dominated by a plastic flow (reduced for large grained ceramics) is considered less damaging in terms of its impact on strength [5]. The microstructure of IPS e.max® CAD when machined is composed of a ~40 vol.% of ~0.5 μm grain-size, lithium-metasilicate crystalline phase in a lithium disilicate glass [21]. Vita Suprinity® and Celtra® Duo consist of lithium silicate glass with 10% dissolved zirconia and contain diphosphorus pentoxide to nucleate lithium metasilicate crystallization. Whereas Vita Suprinity® is machined in a pre-crystallized form containing only an ultrafine lithium metasilicate crystalline phase, Celtra® Duo is machined with a fully developed microstructure comprised of ~1 μm length lithium metasilicate crystals, surrounded by nanometric lithium orthophosphate crystals in a residual glass matrix [23,24]. Although the exact pattern of material removal cannot be discriminated, it can be surmised that prior to heat treatments the three lithium silicate ceramics possessed differences in surface defect integrals and in residual stresses. It is proposed that damage accumulation in Celtra® Duo would be the most dissimilar, given the higher crystalline fraction and larger grain size. Vita Suprinity® and Celtra® Duo have similar composition and microstructure in the fully crystallized form, and in this study, the BFS of the control samples polished after crystallization were similar. The difference in BFS, with CAD–CAM Celtra® Duo significantly weaker can therefore be primarily attributed to differences in initial damage accumulation associated with machining.

In the current study, it is evident that surface cracks and residual stress states introduced by machining were not eliminated by post-processing heat treatments applied for either microstructure development (IPS e.max® CAD and Vita Suprinity®) or annealing/crack blunting (Celtra® Duo). SEM images of fracture surfaces shows median and lateral cracks peripheral to the fracture origin which generally appeared to extend a greater depth in low BFS Vita Suprinity® and Celtra® Duo specimens. At the fracture origins lateral cracks were clearly identifiable in most cases (Fig. 5) and appear to have extended parallel to the specimen surface suggesting the presence of residual stress fields localized within a region near the machined surface. The least surface damage was evident for CAD–CAM IPS e.max® CAD specimens which exhibited the highest BFS. Although IPS e.max® CAD and Vita Suprinity® are machined in a somewhat similar pre-crystallized state, Vita Suprinity® exhibited a large variance in BFS when compared with IPS e.max® CAD. This observation is consistent with a previous finding when high variation in flexural strength of Vita Suprinity® was observed [24]. The authors reported microcracking throughout the test specimens following crystallization and concluded that a mismatch in thermal expansion of the crystalline and glassy phases was responsible [24]. SEM image of fracture surfaces of both Vita Suprinity® and Celtra® Duo (Fig. 5) show some evidence of isolated cracks distant from the sample surface which may support the previous observations [24].

5. Conclusions

The current study demonstrates that chair-side CAD–CAM of lithium silicate glass-ceramics introduces surface damage which limits material strength. Post-processing steps including crystallization and annealing heat treatments are likely to modify strength limiting defects and residual stress states, but do not eliminate the surface damage introduced at the time of machining. A simplified disk geometry for ball-on-ring biaxial flexural testing was used to replicate the clinical stress state expected at machined inner 'fit' restoration surfaces and to allow analytical prediction of failure stress. However, it is acknowledged that in vivo there is a more complex geometry and stress distribution within the restoration. The experimen-

tal method used here was quasi-static in nature, and further work should be conducted to consider the dynamic nature of loading encountered during masticatory function.

Acknowledgments

N.R. and S.V. were funded by the BioTalent Canada Student Workplace Program. The work was supported by the University of Alberta Fund for Dentistry.

REFERENCES

[1] Mormann WH. The evolution of the CEREC system. J Am Dent Assoc 2006;137:7–13.
[2] Li RW, Chow TW, Matinlinna JP. Ceramic dental biomaterials and CAD/CAM technology: state of the art. J Prosthodont Res 2014;58:208–16.
[3] Marshall DB, Evans EG, Khuri Yakub BT, Tien JW, Kino GS. The nature of machining damage in brittle materials. Proc R Soc Lond 1983;385:461–75.
[4] Zhang GM, Satish KG, Ko WK. The mechanics of material removal mechanisms in machining ceramics. Technical report TR 94-22rl. Maryland: Institute for Systems Research (NIST); 1994.
[5] Hu KX, Chandra A. A fracture mechanics approach to modelling strength degradation in ceramic grinding processes. J Eng Ind 1993;115:73–83.
[6] Xu HK, Jahanmir S. Microfracture and materials removal in scratching of alumina. J Mater Sci 1995;30:2235–47.
[7] Le DT. Optimization of machining performance of dental ceramic restorative materials. MS 97-1. Maryland: University of Maryland; 1997.
[8] Apel E, Deubener J, Bernard A, Höland M, Müller R, Kappert H, et al. Phenomena and mechanisms of crack propagation in glass-ceramics. J Mech Behav Biomed Mater 2008;1:313–25.
[9] Quinn GD, Giuseppetti AA, Hoffman KH. Chipping fracture resistance of dental CAD/CAM restorative materials: part I, procedures and results. Dent Mater 2014;30:e99–111.
[10] Malkin S, Ritter JE. Grinding mechanisms and strength degradation for ceramics. J Eng Ind 1989;111:167–74.
[11] Rice RW, Mecholsky JJ. The nature of strength controlling machining flaws in ceramics. Washington, DC: NBS Special Publication: The Science of Ceramic Machining and Surface Finishing II. US Government Printing Office; 1979.
[12] Addison O, Cao X, Sunnar P, Fleming GJP. Machining variability impacts on the strength of a 'chair-side' CAD-CAM ceramic. Dent Mater 2012;28:880–7.
[13] Rice RW, Mecholsky JJ, Becher PF. The effect of grinding direction on flaw character and strength of single and polycrystalline ceramics. J Mater Sci 1981;16:853–62.
[14] Conway JC, Kirchner HP. The mechanics of crack initiation and propagation beneath a moving sharp indenter. J Mater Sci 1980;15:2879–83.
[15] Tapie L, Lebon N, Mawussi B, Fron-Chabouis H, Duret F, Attal JP. Understanding dental CAD/CAM for restorations—accuracy from a mechanical engineering viewpoint. Int J Comput Dent 2015;18:343–67.
[16] Sindel J, Petschelt A, Grellner F, Dierken C, Greil P. Evaluation of subsurface damage in CAD/CAM machined dental ceramics. J Mater Sci Mater Med 1998;9:291–5.
[17] Rekow D, Thompson VP. Near-surface damage—a persistent problem in crowns obtained by computer-aided design and manufacturing. Proc Inst Mech Eng H 2005;219:233–43.
[18] Fraga S, Valandro LF, Bottino MA, May LG. Hard machining, glaze firing and hydrofluoric acid etching: do these procedures affect the flexural strength of a leucite glass–ceramic? Dent Mater 2015;31:e131–40.
[19] Isgró G, Addison O, Fleming GJP. Transient and residual stresses in a pressable glass-ceramic before and after resin-cement coating determined using profilometry. J Dent 2011;39:368–75.
[20] Isgró G, Addison O, Fleming GJP. Deformation of a dental ceramic following adhesive cementation. J Dent Res 2010;89:87–90.
[21] Hallmann L, Ulmer P, Kern M. Effect of microstructure on the mechanical properties of lithium disilicate glass-ceramics. J Mech Behav Biomed Mater 2018;82:355–70.
[22] Timoshenko S, Woinowsky-Krieger S. Symmetrical bending of circular plates. In: Theory of plates and shells. 2nd ed. New York: McGraw-Hill; 1959.
[23] Belli R, Wendler M, de Ligny D, Cicconi MR, Petschelt A, Peterlik H, et al. Chairside CAD/CAM materials. Part 1: measurement of elastic constants and microstructural characterization. Dent Mater 2017;33:84–98.
[24] Wendler M, Belli R, Petschelt A, Mevec D, Harrer W, Lube T, et al. Chairside CAD/CAM materials. Part 2: flexural strength testing. Dent Mater 2017;33:99–109.
[25] Isgró G, Addison O, Fleming GJP. Transient and residual stresses induced during the sintering of two dentin ceramics. Dent Mater 2011;27:379–85.
[26] Furtado de Mendonca A, Shahmoradi M, Gouvêa CVD, De Souza GM, Ellakwa A. Microstructural and mechanical characterization of CAD/CAM materials for monolithic dental restorations. J Prosthodont, 10.1111/jopr.12964. [in press].
[27] Kelly JR. Clinically-relevant approach to failure testing of all-ceramic restorations. J Prosthet Dent 1999;81:652–61.
[28] Lebon N, Tapie L, Vennat E, Mawussi B. Influence of CAD/CAM tool and material on tool wear and roughness of dental prostheses after milling. J Prosthet Dent 2015;114:236–47.
[29] Denry IL, Holloway JA, Tarr LA. Effect of heat treatment on microcrack healing behaviour of a machinable dental ceramic. J Biomed Mater Res 1999;48:791–6.